RESPONSE SURFACE METHODOLOGY TO MODEL THE PROJECTED SPRAY METAL TRANSFER IN GMAW

Jesús E. Pinto Lopera, jesusemilio@unb.br
Sadek C. Absi Alfaro, sadek@unb.br
University of Brasília, Departament of Mechanical Engineering, Brasília, D.F., 70.910-900, Brazil

Abstract. *Response surface methodology (RSM) has been used to obtain an empirical model for describe the droplet size and transfer rate behavior in projected spray metal transfer for gas metal arc welding (GMAW). For a constant voltage power source, the model responds to variations in wire feed rate and voltage; other parameters such as shielding gas mixture and electrode-wire diameter has been kept constant. The model was obtained from the droplets size and transfer rate data collecting from specific value of wire feed rate and voltage. The data came from back-lighting techniques, high-speed camera and images processing algorithms. The model response is in a good agreement with the experimental data and shows a stability relation between input and output system parameters.*

Keywords*: GMAW, projected spray, empirical model, response surface methodology, digital image processing.*

1. INTRODUCTION

Gas Metal Arc Welding (GMAW) is currently the most widely used arc welding process in industry. The process uses a continuously-fed filler metal electrode, and carries benefits such as high production rates and eases automation. A variant of GMAW process uses metal cored wires (MC), which are tubular wires filled with metallic powders to make up the bulk of the core materials. While their construction resembles flux cored wires, metal cored wires are much closer to solid wires in performance and usability. In recognition of these similarities, metal cored wires have been classified and placed within the specifications dealing with solid wires for gas metal arc welding (Lyttle, 1996).

All commercially important metals such as carbon steel, high-strength low alloy steel, stainless steel, aluminum, copper, titanium, and nickel alloys can be welded in all position with GMAW process by choosing appropriate shielding gas, electrode, and welding variables (Weglowski, 2008). This choosing is also important because the metal transfer modes depend on it. This influence the penetration, bead morphology, process stability and spatter. The modes under the natural metal transfer class in GMAW process are presented in tow groups: *contact* (short circuiting) and *free flight*. *Projected Spray* transfer mode belongs to the latter one. This transfer is characterized by high currents and deep penetration in to the base material, the arc is stable and the process is spatter-free.

In general, welding parameters must be set properly, seeking, at the end, a weld bead with good looks and high quality. To find the best parameters, one can use mathematical models for finding answers from different input variables. The models design is performed using a theoretical approach, as in the static force balance theory, or empirical, which are determined from the statistical analysis of different experiments. The complex correlation among the factors involved in metal transfer and its influence in the responses make the theoretical models limited in the use of parameters, by which the experimental study still maintains its importance. The empirical models are obtained through the study of experimental parameters and their effects in certain processes. These models are often used to find the parameters combination that generates the best responses or to describe the physical phenomena that occur in the process. One of the most appropriate processes to find empirical models is the response surface methodology (RSM). Benyounis and Olabi (2008) make a bibliographical study in different welding processes and highlight the interest in models based on RSM and the potential they have in parameters optimization to generate safe and economical welding processes with good appearance and good quality.

This paper presents two empirical models to represent the metal transfer behavior in projected spray mode. The models were established from an experimental design based on response surface methodology and study two fundamental parameters, droplet size and droplet transfer rate. To develop the models, measure these parameters in different welding processes was necessary. The measurement was made using a computer program developed in this work which is based on digital image processing. To perform the corresponding measurements, was used filming of metal transfer in different welding experiments. Filming was done with a high speed camera and back-lighting technique. Thus one can study the droplet formation and detachment process and quantify the size of these when they are in flight between the wire and work piece.

2. PROJECTED SPRAY TRANSFER

Projected Spray is associated with high currents and high temperatures, in general its use is limited to plates with thickness larger than 3 mm, where it is effective for producing a high penetration. The transfer occurs primarily with shielding gas based in argon and with positive electrode. The transfer mode is characterized by small and uniform droplets transfer (with diameter close to the electrode size) in high frequency rate (at a rate of hundreds per second). As

the droplets go one after the other, the term spray is misused, but universally applied to describe this transfer (Ponomarev *et al.*, 2009). The IIW (International Institute of Welding) determined that, in spray transfer, the droplet diameter is less than 1.25 times electrode diameter (Iordachescu *et al*., 2006). The process has high arc stability and the arc voltage and welding current oscillograms do not differ significantly. As the welding current increases, the droplet size decreases and the transfer rate increases. For spray transfer occurs, the welding current must exceed a current range named transition current, which depends on several input factors including the electrode size, composition and shielding gas type.

2.1. Droplet formation

In the GMAW process studies different theoretical models have been proposed in order to describe the droplets process formation and to predict parameters (*responses*) as droplet diameters, rate transfer, transition currents, among others. The two most well-known models of metal transfer are the static force balance theory and the pinch instability theory. Currently, the models agree that electromagnetic forces dominate the droplet formation when the welding current exceeds the transition current. Lowke (2009) concludes that spray transfer transition occurs when the pressure, from the self magnetic field of the current inside the molten drop, exceeds the surface tension pressure produced by the radius of the wire.

Scotti and Ponomarev (2008) describe that current density through the wire, and magnetic field around it, will produce radial forces towards the wire center. These forces are named the *Lorentz force* (F_L). For a solid conductor, the effect of this force can be neglected, but for a liquid conductor (as molten metal drops at the wire tip), the Lorentz forces shift the surface to conductor center. Thus, in opposite direction to electrode, the drop tends to lengthen and the diameter decreases at molten drop coupling with the wire (*neck-shrink*, Fig. 1). This is called the *Pinch effect*, and based on it, this work made wire diameter measurements to determine the drop formation and detachment in order to estimate the droplet transfer rate in the process.

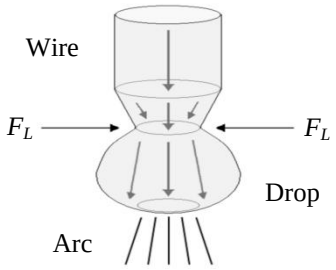

Figure 1. Pinch effect illustration; the arrows through the wire indicate the current flow (adapted from Scotti and Ponomarev, 2008).

3. RESPONSE SURFACE METHODOLOGY (RSM)

The response surface methodology is a set of mathematical and statistical techniques used to model processes in which responses are influenced by different independent variables (*input variables*). The generated model is a mathematical equation that estimates process responses according to input variables within a work region. The graphical obtained from this model is the response surface and indicates the behavior of responses in function of input variables. One of the most important experimental designs in RSM is the c*entral composite design* (CCD). Presented in Fig. 2, CCD is widely used for fitting a second-order response surface. The design consist of a tow-level factorial design (the corners of the square), plus four axial runs, plus four runs at the center of work region (center of the square).

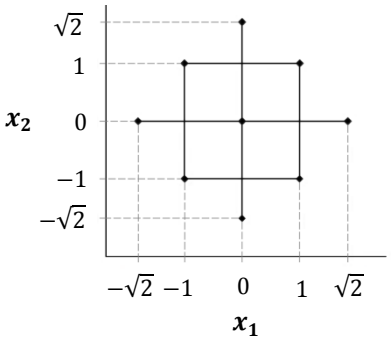

Figure 2. Central composite design for two input variables (x_1,x_2).

The units in Fig. 2 represent the coded variables, which are the difference between the variables and the center of the analysis region. They need to be coded because the differences between units of variables measurement can influence the model responses. Input variables are encoded using the following expression:

$$x_j = \frac{\xi_j - (\max(\xi_j) + \min(\xi_j))/2}{(\max(\xi_j) - \min(\xi_j))/2} \tag{1}$$

, where x_j indicates the coded variable and ξ the real value of the input variable, j represents the input variable, $\max(\xi_j)$ and $\min(\xi_j)$ are the real values of input variables in the factorial design (the corners in Fig. 2). The initial model responses are given in terms of coded variables, so Eq. (1) is used to translate the answers to real values of the model (final model).

3.1. Multiple linear regression model

To establish the model in response surface methodology, Myers *et al*. (2009) use multiple linear regression technique. For the case of a second order model, this has the form:

$$y = \beta_0 + \beta_1 x_1 + \beta_2 x_2 + \beta_{11} x_1^2 + \beta_{22} x_2^2 + \beta_{12} x_1 x_2 + \varepsilon \tag{2}$$

, where y represents the response, x the input variable and ε the model random deviation and it is assumed that this is a normal distribution with zero mean and variance σ^2. The β–terms represent the parameters that determine the model and are called *regression coefficients*. The term "linear" is used because Eq. (2) is a linear function of the unknown regression coefficients, regardless the shape of the response surface that it generate.

3.2. Estimation of the regression coefficients

The method of last squared is typically used to estimate the regression coefficients in a multiple linear regression model. In general, the experimental design can be developed as indicated in Tab. 1.

Table 1. Experimental design ($n > k$).

Observation	x_1	x_2	⋯	x_j	⋯	x_k	y
1	x_{11}	x_{12}	⋯	x_{1j}	⋯	x_{1k}	y_1
2	x_{21}	x_{22}	⋯	x_{2j}	⋯	x_{2k}	y_2
⋮	⋮	⋮		⋮		⋮	⋮
i	x_{i1}	x_{i2}	⋯	x_{ij}	⋯	x_{ik}	y_i
⋮	⋮	⋮		⋮		⋮	⋮
n	x_{n1}	x_{n2}	⋯	x_{nj}	⋯	x_{nk}	y_n

, where n is the number of observations and k is the number of input variables; y_1, y_2,..., y_n are the experiments responses, y_i is the i-th response and x_{ij} is the coded variable x_j in the i-th observation of variable j. For second order models, $k = 5$; $x_3 = x_1^2$; $x_4 = x_2^2$ and $x_5 = x_1 x_2$. Using Table 1 in the following expressions:

$$\boldsymbol{y} = \begin{bmatrix} y_1 \\ y_2 \\ \vdots \\ y_n \end{bmatrix}, \qquad \boldsymbol{X} = \begin{bmatrix} 1 & x_{11} & x_{12} & \cdots & x_{1k} \\ 1 & x_{21} & x_{22} & \cdots & x_{2k} \\ \vdots & \vdots & \vdots & & \vdots \\ 1 & x_{n1} & x_{n2} & \cdots & x_{nk} \end{bmatrix} \tag{3}$$

The way to find the regression coefficients (β's) is doing:

$$\boldsymbol{b} = (\boldsymbol{X}^T \boldsymbol{X})^{-1} \boldsymbol{X}^T \boldsymbol{y} \tag{4}$$

, where $\boldsymbol{b}$ is the column vector with (k + 1) positions that contains the estimators of regression coefficients. Thus the second order model can be written as:

$$\hat{y} = b_0 + b_1 x_1 + b_2 x_2 + b_3 x_1^2 + b_4 x_2^2 + b_5 x_1 x_2 \tag{5}$$

The difference between the observation y_i and the fitted value $\hat{y}_i$ is the *residual* and is denoted by:

$$e_i = y_i - \hat{y}_i \tag{6}$$

An effective approach to evaluate the model accuracy is to calculate the predicted response ($\hat{y}_i$) and the residuals (e_i) to graph some of the calculated quantities. Graphics are examined to confirm the model or to get indications that the model is not appropriate. The graphics can be y_i versus $\hat{y}_i$ and e_i versus $\hat{y}_i$, the normal probability plot of the residuals, among other. To estimate the model variance (σ^2), multiple regression consider the sum of squares of the residual ($\sum_{i=1}^{n} {e_i}^2$), so called the *residual sum of squares* (SS_E). As $k + 1$ parameters (b_0, b_1, ..., b_k) have been estimated, $k + 1$ degrees of freedom (*df*) are lost, so $n - (k + 1)$ *df* is associated with SS_E, and

$$\hat{\sigma}^2 = s^2 = \frac{\sum_{i=1}^{n}(y_i - \hat{y}_i)^2}{n - (k+1)} \tag{7}$$

The amount of reduction in the variability of *y* obtained by using the regressor variables $x_1, x_2, \ldots, x_k$ in the model is named the *adjusted coefficient of multiple determination* (R_{adj}^2) defined as:

$$R_{adj}^2 = 1 - \frac{n-1}{n-(k+1)} \cdot \frac{\sum_{i=1}^{n}(y_i - \hat{y}_i)^2}{\sum_{i=1}^{n}(y_i - \bar{y})^2} \tag{8}$$

, where, $\bar{y}$ is the sample mean of measurements.

4. DIGITAL IMAGE PROCESSING

Digital image processing is a general term for the wide range of techniques that exist for manipulating and modifying digital image in various ways. Digital images processing covers different topics, from image acquisition to results interpretation. In this paper we discuss some of the most common.

4.1. Back-lighting illumination

Back-lighting is an illumination technique used with high-speed cameras to filming metal transfer in GMAW welding processes. The technique uses directional back-lighting illumination with a laser beam as light source. General overview of technique is presented in Fig. 3. The lens system propagates the beam expander to interest objects and direct to the camera. Before reaching the camera lens, the laser beam passes through an optic band-pass interference filter (in laser band), then the arc light that not coincide with the filter band are rejected.

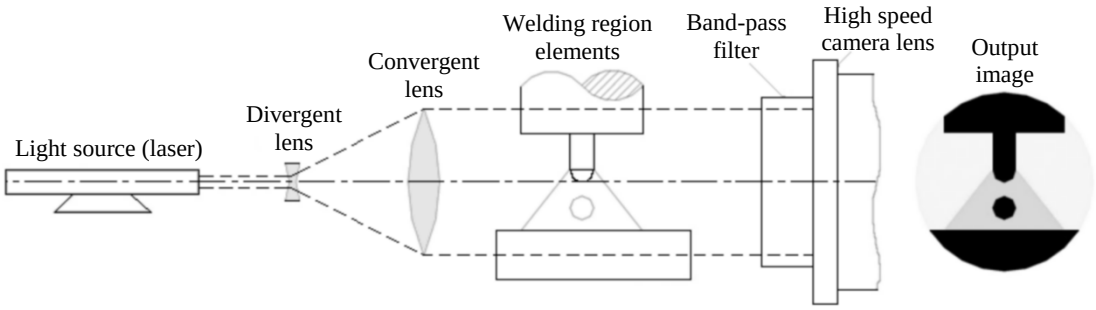

Figure 3. The principle of back-lighting applied to welding (Bálsamo et al, 2000).

4.2. Image enhancement

In image enhancement, the goal is to process an image with a result more suitable than original for a specific application. Some topics in image enhancement include contrast and edge enhancement, noise filtering, sharpening, and magnifying. For example, Maia (2001) used spatial smoothing filters for image processing of metal transfer. Spatial domain methods are procedures that operate directly on the image pixels. Two examples are *Gaussian smoothing* and *median* filters. Trucco and Verri (1998) show algorithms to develop each filter.

4.3. Thresholding

The technique of thresholding is used in image segmentation. Thresholding transforms a set of pixels containing values that vary over some range into a new set containing just two values. It does this by applying a threshold, *T*, to the input set. Input values that fall below the threshold are replaced by one of the output values; input values at or

above the threshold are replaced by the other output value. Because there are two possible output values, thresholding creates a binary image (usually black and white). Weska (1978) classifies the methods of thresholding into three groups: global, local and dynamic. When *T* depends only on image intensity (gray-level values) the threshold is called global. If *T* depends on both image intensity and some spatial information of image (a region), the threshold is called local. If, in addition, T depends on the spatial coordinate, the threshold is called dynamic.

4.4. Labeling

Once the image objects are separated from the background, it is necessary to distinguish them from each other. For this, all pixels that belong to the same object will be identified with the same label (in this case, the label is a gray-level). This process is known as labeling and is based on connectivity between pixels of the same object as described in Lopera and Muñoz (2007). With the objects labels is possible to make any type of measure (in pixels units) on the objects.

5. METHODOLOGY

According to Lopera (2010), modeling of projected spray metal transfer was designed using multiple linear regression and is composed by two second order models, corresponding to droplet size and transfer rate. The experimental design is based on central composite design. The measurement of size and transfer rate is done by algorithms of digital image processing applied to image sequences of the process.

5.1. Experimental design

For central composite design were selected nine work points within the spray projected transfer area. Since measured responses depend on a lot of parameters such as shielding gas composition or electrode wire diameter, in this study the experiments were established solely to changes in voltage and wire feed rate, traditional control factors of a constant voltage power source, the others input factors were kept constant. Agree with bibliography, the work convenience and the equipment characteristics, it was defined to work with: positive polarity; electrode tip and work piece distance, 18 mm; shielding gas flow rate, 14 liters/min (measured at cylinder outlet); welding speed, 10 mm/s; right angles between electrode and work piece.

Agree with availability of the laboratory, the materials used in this study were: electrode, *410NiMo MC* with 1.2 mm diameter; base material, *1020 steel* with flat-plate shaped, 6 mm thickness, 200 mm length, 50 mm width; shielding gas, *Stargold Plus*. The powers source used was *Fronius TransPuls Synergic* in constant voltage mode. From metal transfer films of different experiments with different input parameters, limits of work region were established as:

- Wire feed rate (ξ_1) between 5.7 and 7.3 m/min;
- Voltage (ξ_2) between 26.5 and 29.5 V.

The work region center point is (ξ_1, ξ_2) = (6.5 m/min, 28 V). The values of two-level factorial design are 6 and 7 m/min for wire feed rate, and, 27 and 29 V for work voltage. Values corresponding to coded variables $\pm\sqrt{2}$ (for axial runs) are rounded in order to use them in the power source.

5.2. Images processing

To develop the methodology and measure the characteristics of each work point, it was analyzed sequences of 100 images corresponding to 100 ms welding time. The transfer rate is calculated by counting the drops that are transferred to weld pool during that time. Droplet size is calculated as diameter of transferred droplets. The image processing methodology makes use of the following:

- Image acquisition
- Image enhancement
- Image thresholding
- Labeling
- Size droplet measurements
- Transfer rate measurements

Images used for measurement were taken from videos made with a CMOS high speed camera (DALSA model DS-21-001M150), the sampling rate was 1000 frames per second at a resolution of 180x96 pixels and 256 gray levels. The back-lighting was the illumination technique used. The welding experiments were made in a time of 6 seconds. Thus, we obtained image sequences like the one shown in Fig. 4.

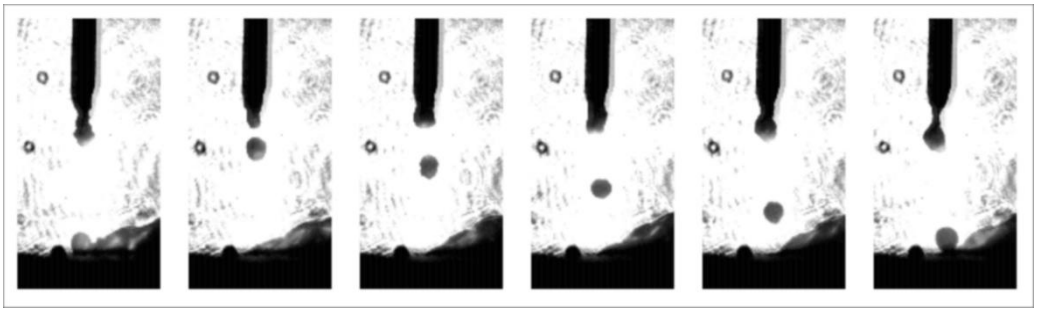

Figure 4. 6 images sequence of projected spray transfer video. 1000 frames/s sampling rate.

The images enhancement is made using a Gaussian smoothing and median filters, each built with a mask of size 3x3 pixels. The Gaussian filter is proposed to soften the image and reorganize the value of pixels in accordance with its neighbors. The median filter is used to eliminate isolated pixels, separating large areas of noise (many noise regions are composed of isolated pixels chains). Images thresholding is done using the *Otsu* method (Otsu, 1979), which allows automatically find the appropriate threshold for each image. In this work, the thresholding is performed in two steps: global and dynamic (according to classification of Weska, 1978). In the first stage, interests are focused on eliminating the noise and identify the main element in the picture, the wire. The second stage makes a thresholding in the arc zone where the interest is the droplet and other thresholding in the wire tip to transfer rate calculation. For this, the objects labeling is used, because first one has to find space coordinates (pixels) of wire tip and weld pool within the image.

The labeling is done by scrolling through the image pixel by pixel, from left to right and from top to bottom. The assessment of connectivity is made with the 8-adjacency. In some cases, after making the first labeling process, some objects may have two or three different labeling, which makes necessary a process of labels equalization on objects. Thus, objects are fully identified, making it possible to count and record the coordinates of each of its pixels, allowing defining the size and spatial location of each object. In this step, the noises that were not fully eliminated on thresholding are removed from the image by comparing their size with the weld pool size. A detailed study on hundreds of images indicated that each remaining noise size does not exceed 3% of weld pool area. Figure 5 shows the use of labeling in noise elimination.

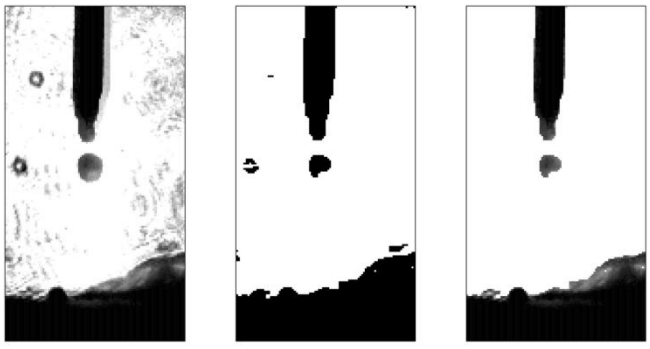

(a) (b) (c)

Figure 5. Sequential processing of one image. (a) Original image; (b) image thresholding; (c) noise removed by size.

To make the dynamic thresholding and to measure the droplet size is necessary to delimit the arc area. For this, one takes the last pixel coordinates (top to bottom) of the wire tip and the first pixel coordinates of the weld pool, which is taken as the first top-down and from left to right (site not influenced by the weld bead) as shown in Fig. 6 (c) and (d). The weld pool is eliminated of the arc area. In this area, it used again the Otsu method, finalizing the second stage thresholding (Fig. 6 (e) and (f)). This step is necessary because the droplets have intermediates gray levels between the clear of background and the dark of wire and weld pool, so in the global thresholding, the droplets are eliminated or lose pixels, as the case in Fig. 6. Making a new threshold only in the arc area, the two groups are the pixels that form the background and the droplet, the remaining noise is removed by size (Fig. 6 (g) and (h)). Usually the wire tip also appears, but it is not considered. In this work, the droplet size is presented as the *droplet diameter* and is measured in pixels. Units conversion (pixels to mm) were not done, but can be made from the proper drop delimitation, as reports Maia (2001) or Weglowski *et al*. (2008).

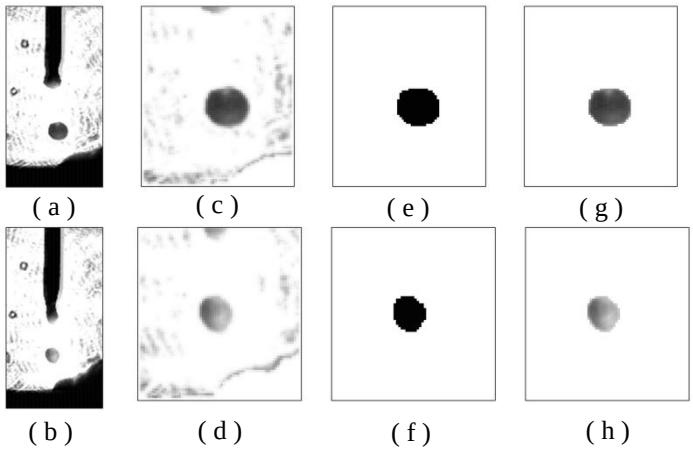

Figure 6. Process to droplet size measurement. (a) and (b) Images transfer; (c) and (d) zone of influence of the arc for their images to the left; (e) and (f) dynamic thresholding; (g) and (h) drop clean for visual comparison.

The diameter calculation depends of a measure named the *droplet area*, which is calculated as the sum of pixels that form the drop. In this work, each droplet diameter (D) was calculated as:

$$D = 2\left(\sqrt{\frac{droplet\ area}{\pi}}\right) \tag{9}$$

To measure the droplet transfer rate is necessary to count the number of droplets that are transferred in the process during a fixed time, in this case 100 ms. In order to achieve this goal, a new thresholding is done around the wire tip, which lets recover the points lost by global thresholding process. Then, analyzing the wire tip, frame by frame, looking to follow the process of neck-shrink produced by Pinch effect. In formation process, the droplet is attracted and moved to weld pool, and before the transfer the neck can reach a length close to the wire diameter. Thus, an analysis region is chosen with twice wire diameter length, where his last line coincides with the last pixel of the wire tip, as shown in Fig. 7. To know if a drop was detached, are performed measurements of neck and drop diameter over this region.

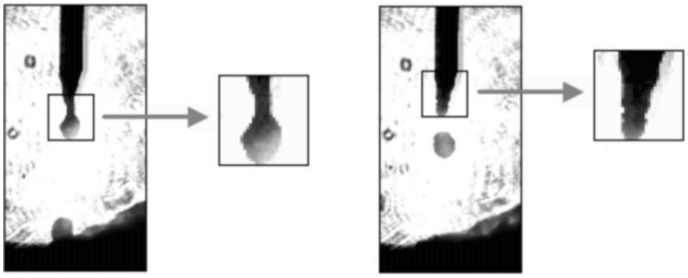

Figure 7. Analysis region to calculate the droplet transfer rate. Two different images.

Images analysis indicated there are two bands of pixels within the analysis region suitable to take diameter measurements. The first, to measure the neck, is located around the quarter of analysis region (1/4), and the second, to measure the droplet, is located around three quarters of region (3/4) as shown in Fig. 8. In this case, the word "diameter" refers to sum of pixels contained in four rows of image located in the ranges indicated. When the droplet is being formed and the neck is manifest, the number of pixels located in the first band is less than the number of pixels that are in the second band, as shown in Fig 8 (a). After droplet transfer, the result is opposite, as shown in Fig. 8 (b). A comparison and follow-up of bands indicates the droplets transfer rate in the welding process.

In this stage we counted the number of drops that left the wire at a time of 100 ms. Another step is to repeat this process a certain number of times to understand the behavior of measures and thus ensure the use of them in model design. So, searching for a large sample, it was decided to repeat the measurement process 70 times for each experiment and get the sample mean.

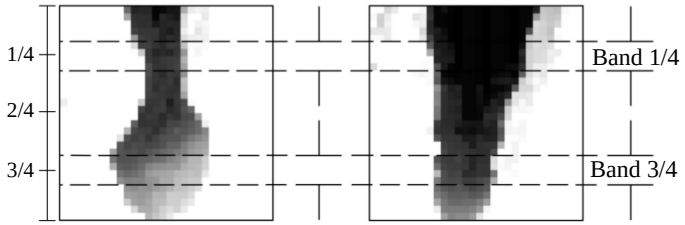

Figure 8. Bands to calculate the transfer rate. (a) Wire tip with droplet formation, (b) wire tip after droplet transfer.

6. RESULTS

Table 2 presents the experimental design and results of area, diameter and transfer rate measures for every work point in reference to input and coded variables. Each response data is a sample mean of 5 measures in the work point. Each transfer value was multiplied by 10 to get an approximate value to a second.

Table 2. Experimental design for droplet size and transfer rate

Observation	Coded variables		Input variables		Responses/measures		
	x_1	x_2	Wire feed rate (ξ_1) (m/min)	Voltage (ξ_2) (V)	Area (Pixels)	Diameter (Pixels)[(1)]	Transfer rate (Droplets/s)
1	-1	-1	6	27	263.97	18.27	123.34
2	1	-1	7	27	225.93	16.93	174.94
3	-1	1	6	29	241.60	17.51	124.40
4	1	1	7	29	189.84	15.52	215.77
5	$-\sqrt{2}$	0	5.8	28	256.43	17.87	116.5
6	$\sqrt{2}$	0	7.2	28	199.39	15.90	218.65
7	0	$-\sqrt{2}$	6.5	26.6	237.64	17.37	142.51
8	0	$\sqrt{2}$	6.5	29.4	196.26	15.78	183.48
9	0	0	6.5	28	226.11	16.94	158.28
10	0	0	6.5	28	228.16	17.02	155.14
11	0	0	6.5	28	226.59	16.96	156.00
12	0	0	6.5	28	225.68	16.92	159.57

(1): To compare, the wire diameter measured in images is 16 pixels.

Referring to Eqs. (1), (3), (4) and (5), and the experimental design (Table 2), the droplet diameter second-order model is:

$$\hat{y}_D = -95.9874 + 5.2622\xi_1 + 7.7538\xi_2 + 0.1776\xi_1^2 - 0.1106\xi_2^2 - 0.325\xi_1\xi_2 \quad (10)$$

, for droplet transfer rate is:

$$\hat{y}_{TR} = 4737.27 - 679.78\xi_1 - 198.5\xi_2 + 15\xi_1^2 + 1.46\xi_2^2 + 19.88\xi_1\xi_2 \quad (11)$$

In order to calculate the model behavior, are used equations (7) and (8) to calculate the variance ($\hat{\sigma}^2$) and the adjusted coefficient of multiple determination percentage ($\%R^2_{adj} = 100 \cdot R^2_{adj}$). To diameter model:

$$\hat{\sigma}^2{}_D = 0.043; \quad \%R^2_{adj_D} = 94\% \quad (12)$$

To droplet transfer rate model:

$$\hat{\sigma}^2{}_{TR} = 18.21; \quad \%R^2_{adj_{TR}} = 98.35\% \quad (13)$$

Making use of Eq. (6), Table 3 shows the model residuals at each work point. Figure 9 presents normal probability plots of residuals for each model. Plots show the residuals distributed along the straight line that forming a normal distribution, allowing to show a good indication that the model is a satisfactory fit to the data.

Table 3. Residuals to droplet size and transfer rate models

Observation	Wire feed rate (ξ_1) (m/min)	Voltage (ξ_2) (V)	**Diameter (Pixels)**			**Transfer rate (Droplets/s)**		
			Experiment measure	Model response	Residual	Experiment measure	Model response	Residual
1	6	27	18.27	18.05	0.22	123.34	123.98	-0.64
2	7	27	16.93	16.84	0.09	174.94	175.96	-1.02
3	6	29	17.51	17.27	0.24	124.40	129.06	-4.66
4	7	29	15.52	15.41	0.11	215.77	220.80	-5.03
5	5.8	28	17.87	18.13	-0.26	116.5	113.93	2.57
6	7.2	28	15.90	15.97	-0.07	218.65	215.55	3.10
7	6.5	26.6	17.37	15.52	-0.15	142.51	142.51	0.00
8	6.5	29.4	15.78	15.96	-0.18	183.48	177.81	5.67
9	6.5	28	16.94	16.96	-0.02	158.28	157.25	1.03
10	6.5	28	17.02	16.96	0.06	155.14	157.25	-2.11
11	6.5	28	16.96	16.96	0.00	156.00	157.25	-1.25
12	6.5	28	16.92	16.96	-0.04	159.57	157.25	2.32

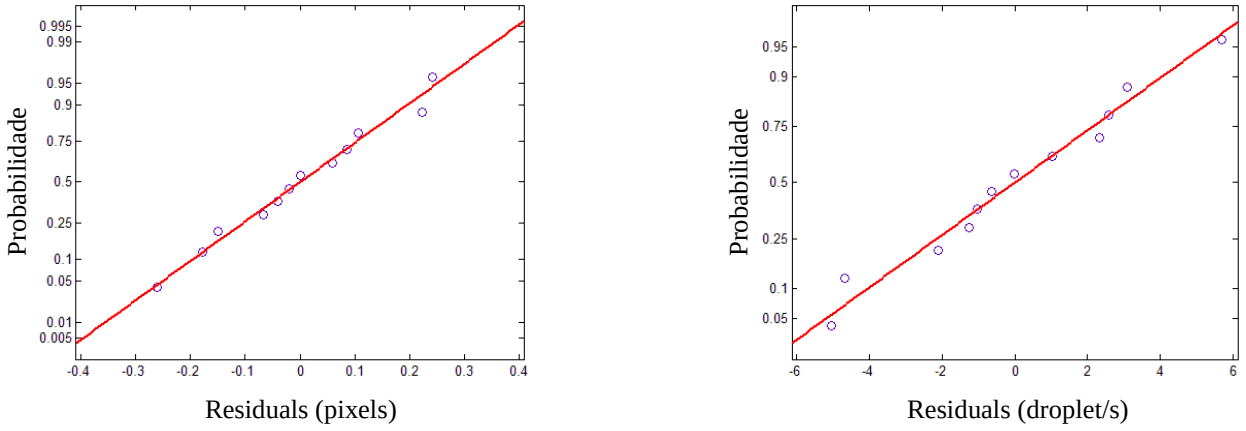

(a) (b)

Figure 9. Normal probability plot of residuals. (a) Droplet diameter; (b) transfer rate.

Figure 10 shows a view of response surface generated by the droplet diameter and transfer rate models as a function of input variables.

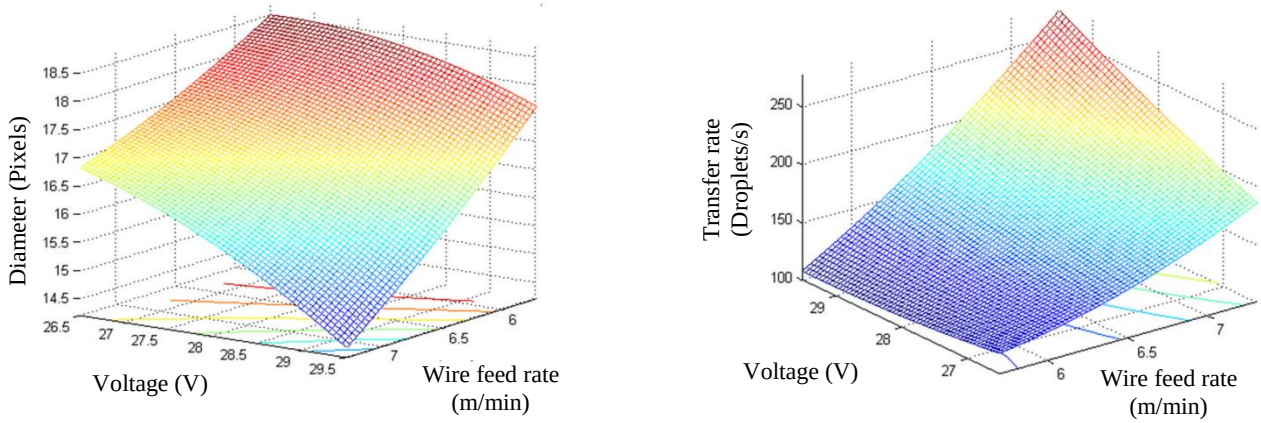

(a) (b)

Figure 10. Response surface of models. (a) Droplet diameter; (b) transfer rate.

Response surfaces in Fig. 10 allow to observe that, when the input variables value increases the droplet size decreases and transfer rate increases, which, agree to bibliography review, both cases suppose a welding current increase. By increasing the wire feed rate, the current increases and thus preserves the balance between wire fusion and

feeding rate. Increasing in voltage increases the arc length, then, electrode extension decreases and thus the heat produced by Joule effect also decreases, so, current increases to maintain the balance between fusion rate and wire feed.

7. CONCLUSION

This paper presents two models corresponding to droplet size and transfer rate. The models were calculated using response surface methodology. The inspection of normal probability plots of the residuals (Figure 9) show the residuals plot approximately along a straight line, revealing no apparent problem with normality. Models of droplet size and transfer rate explain about 94% and 98%, respectively, of the variability observed in the responses. By these percentages and observations in normal probability plots, the models are adequate to describe the projected spray metal transfer.

In reference to digital images processing, the correct segmentation of wire in global thresholding is the most important step in processing, because from wire tip coordinates are determinate the analysis regions to measure the droplets size and transfer rate. The "neck-shrink" produced by Pinch effect proved to be an appropriate parameter to track and calculate the droplets transfer rate.

8. REFERENCES

Bálsamo, P.S., Vilarinho, L.O., Vilela, M. and Scotti, A., 2000. "Development of an Experimental Technique for Studying Metal Transfer in Welding: Synchronized Shadowgraphy". International Journal for the Joining of Materials, Vol. 12, No. 1, pp. 1-12.

Benyounis, K.Y. and Olabi, A.G., 2008. “Optimization of Different Welding Processes Using Statistical and Numerical Approaches – A Reference Guide”. Advances in Engineering Software, Vol. 39, pp. 483-496.

Devore, J.L., 2006. “Probabilidade e Estatística para Engenharia e Ciências”. Pioneira Thomson Learning Ltda., São Paulo, Brasil, 692 p.

Iordachescu, D., Lucas, W. and Ponomarev, V., 2006. Reviewing the “Classification of Metal Transfer”. IIW Doc., No. XII-1888-06, 10 p.

Lopera, J.E.P. and Muñoz, G.L.L, 2007. “Sistema Asistido de Segmentación, Clasificación y Conteo de Cromosomas en Metafase para la Elaboración de Cariotipos Basado en Visión Computacional”. Dissertação de graduação, Universidad del Cauca, Popayán, Colombia.

Lopera, J.E.P., 2010. “Modelagem Empírica da Transferência Goticular Projetada em Processos de Soldagem GMAW Baseada em Técnicas de Processamento de Imagens Digitais e Superfícies de Resposta”. Dissertação de Mestrado em Sistemas Mecatrônicos, Departamento de Engenharia Mecânica, Universidade de Brasília, Brasília, DF, 135p.

Lowke, J.J., 2009. “Physical Basis for the Transition from Globular to Spray Modes in Gas Metal Arc Welding”. Journal of Physics D: Applied Physics, Vol. 42, 7p.

Lyttle, K.A., 1996. “Metal cored wires: where do they fit in your future?”. Welding Journal, Vol. 75, pp. 35-40.

Maia, T.C., 2001. “Utilização de Técnicas de Processamento Digital de Imagens no Estudo de Transferência Metálica em Soldagem a Arco Voltaico”. Dissertação de Mestrado, Universidade Federal de Uberlândia, Uberlândia, M-G, Brasil.

Myers, R.H., Montgomery, D.C. and Anderson-Cook, C., 2009. “Response Surface Methodology, Process and Product Optimization Using Designed Experiments”. John Wiley & Sons, Inc. Hoboken, New Jersey, USA, 680 p.

Otsu, N., 1979. “A threshold selection method from gray-level histograms”. IEEE Transactions on Systems, Man and Cybernetics, Vol. 9, No. 1, pp. 62-66.

Ponomarev, V., Scotti, A., Norrish, J. and Lucas, W., 2009. “Metal Transfer Modes in MIG/MAG (GMAW) Welding: Contributions to a New IIW Classification”. In: 62nd Anual Assembly and International Conference of the International Institute of Welding, 2009, Singapore. IIW 2009. Paris : IIW, 2009. v. CD. p. 1-15.

Scotti, A. and Ponomarev, V., 2008. “Soldagem MIG/MAG melhor entendimento, melhor desempenho”. Artliber Editora, São Paulo, Brasil 284 p.

Trucco E. and Verri, A., 1998, “Introductory Techniques for 3-D Computer Vision”, Prentice Hall, Upper Saddle River, NJ, USA, 343 p.

Weglowskid, M., Huang, Y. and Zhang, Y., 2008, “Effect of Welding Current on Metal Transfer in GMAW”, Archives of Materials Science and Engineering, Vol. 33, pp. 49-56.

Weska, J.S., 1978. “A Survey of Thresholding Selection Techniques”. Computer Graphics and Image Processing, Vol. 5, pp. 382-399.

5. RESPONSIBILITY NOTICE

The authors are the only responsible for the printed material included in this paper.